QCD radiation in top quark decay

David Briggs
Clare College, Cambridge
Supervised by Prof. Bryan Webber
High Energy Physics Group, Cavendish

May 2002

The parton shower approximation is formally valid in the limit of soft and collinear gluon emission. For the process of top quark decay, viewed in the top quark rest frame, this corresponds to independent parton showers off the top and bottom quark respectively. In this paper, we consider the contribution to the total cross section arising from the area of phase space not covered by either shower – the dead region. The draft paper of Webber *et al.*[1] lays the foundations for this project. We carry out further analysis of the variables for the first stage of a parton shower. The shape of the dead region is determined by the initial conditions chosen for the two parton showers. The first-order matrix element for the process ($t \to Wbg$) is integrated over the dead region using Monte Carlo methods. We find the contribution from the dead region to be of the order of unity (with a factor of $\alpha_S C_F \pi^{-1}$). We explore the dependence of the integral on the initial conditions chosen for the showers.

Introduction

Top quark-antiquark pairs may be produced in high-energy proton-antiproton collisions. The top quark decays via the weak interaction to the bottom quark (decays into the down or strange quark are also possible, but are suppressed by their respective CKM matrix elements).

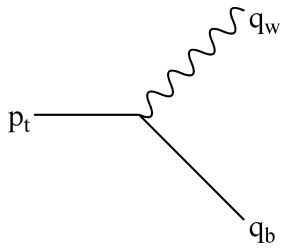

Figure 1, the weak vertex

In this paper, we consider gluon radiation in top decay. The bare process of the quark field coupling to the weak charged field (figure 1) is generally accompanied by photon and gluon emission from the quarks. The weak boson has an very short lifetime and will decay into a positron-neutrino or quark-antiquark pair. All partons will undergo hadronization, producing the hadronic jets observed in the final state.

Gluon radiation and hadronization are phenomena of the strong interaction. In our analysis, we shall use perturbative Quantum ChromoDynamics (QCD) theory. This is valid in the asymptotic region corresponding to large momentum scales for which the running coupling is relatively small. The heavy mass of the top quark, means that we can consider top quark decay a *hard* (large momentum) process.

However, the subsequent process of hadronization, occurring as the momenta of the partons decrease, is a *soft* process. In this region the running coupling is large and perturbative QCD is not valid. This is mentioned as an aside; we will consider gluon radiation in isolation from the process of hadronization.

Confinement means that the study of gluon emission is essential to understanding the final state properties. Hard processes such as top quark decay allow perturbative QCD theory to be tested. Accurate cross section predictions enable the top quark mass to be studied.

Additionally, the top quark is relevant to the search for the Higgs boson. The coupling of the Higgs

field to fermions is proportional to the fermion mass. The top quark/antiquark represents one of the most likely decay channels for a heavy Higgs boson.

Dalitz phase space

To begin, we consider top decay with the emission of a single gluon ($t \to Wbg$). Conservation of momenta imposes the constraint:

$$1) \qquad p_t = q_W + q_b + q_g$$

We constrain the top quark and three final state particles to take their on-shell masses. The heavy top quark allows us to approximate the bottom quark as massless. We shall align our z-axis antiparallel with respect to the *W* boson. The ratio of the *W* and top quark masses gives:

$$2) \qquad a = \frac{m_W^2}{m_t^2} \approx 0.213$$

With these constraints, we can describe the three particle final state in terms of two dimensional phase space. For this, we introduce the Dalitz variables:

$$3) \qquad x_g = 2\frac{q_g . p_t}{m_t^2} \equiv 2\frac{E_g'}{m_t}$$

$$4) \qquad x_w = 2\frac{q_w . p_t}{m_t^2} - a \equiv 2\frac{E_w'}{m_t} - a\,;$$

Evaluated in the top quark rest frame these quantities relate to the fraction of top quark energy carried by the gluon and weak current respectively.

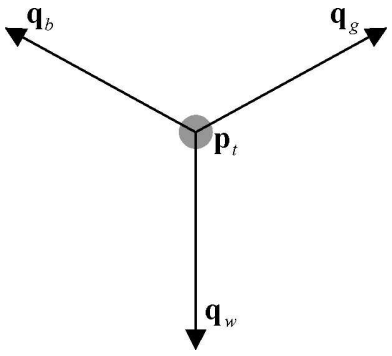

Figure 2, ($t \to Wbg$) observed in top rest frame

To examine the boundaries to phase space, we substitute the Dalitz variables into our constraint (1).

$$\Rightarrow (m_t, \mathbf{0}) = (E_w', \mathbf{q}_w') + (q_b', \mathbf{q}_b') + (q_g', \mathbf{q}_g')$$

$$\Rightarrow m_t = E_w' + \left[q_w'^2 + q_g'^2 + 2q_g' q_w' \cos\theta'\right]^{\frac{1}{2}} + q_g'$$

$$\Rightarrow 2 = (x_w + a) + \left[(x_w + a)^2 + x_g^2 + 2x_g\left\{(x_w + a)^2 - 4a\right\}^{\frac{1}{2}} \cos\theta'\right]^{\frac{1}{2}} + x_g$$

We can consider the two Dalitz variables as functions of the angle, θ', between the gluon and weak current in the top quark rest frame. To find the phase space boundary we solve the equation subject to conditions:

$$\frac{dx_g(\theta')}{d\theta'} = \frac{dx_w(\theta')}{d\theta'} = 0$$

$$\Rightarrow \sin\theta' = 0$$

$$\Rightarrow \theta' = 0 \text{ or } \pi$$

Thus the boundaries of phase space coincide with any two collinear final-state particles. Applying this result to the equation above, we find the condition:

$$5) \qquad 1 - x_g + \frac{a x_g}{1 - x_g} < x_w < 1$$

This defines our allowed phase space in terms of the Dalitz variables.

Fixed first order Perturbative QCD

We now derive the essential features of the first-order matrix element corresponding to top quark decay with single gluon emission ($t \to bWg$). The gluon may be emitted from either quark. We must therefore sum the two corresponding Feynman diagrams, first order in the coupling strength, α_S.

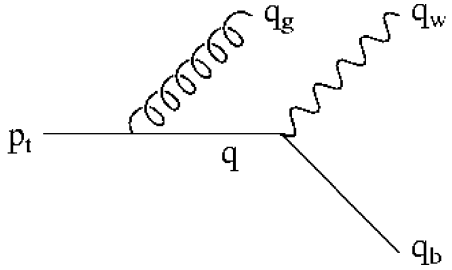

Figure 3, Emission from top

The Feynman rule associated with the top quark propagator (figure 3) gives:

$$6) \qquad \delta_{jl} \frac{i\left(\gamma_\upsilon q^\upsilon + m_t\right)}{q^2 - m_t^2} \propto \frac{1}{-x_g m_t^2}$$

This diverges in the limit $x_g \to 0$, corresponding to *soft* gluon emission (a gluon with zero energy). Without cancellations from other terms in the matrix, this is log-divergent.

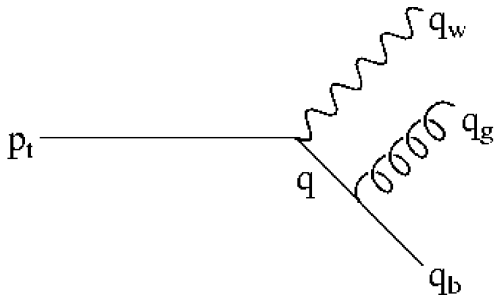

Figure 4, Emission from bottom

The Feynman rule associated with the massless bottom quark propagator (figure 4) yields:

$$7) \qquad \delta_{jl} \frac{i(\gamma_\upsilon q^\upsilon)}{q^2} \propto \frac{1}{(1-x_w)m_t^2}$$

Likewise, this also produces a log-divergence in the limit, $x_w \to 1$, corresponding to gluon emission collinear with the bottom quark.

Summing the two matrix elements for these diagrams, we find the partial differential cross section[1] (see figure A1):

$$8) \qquad \frac{1}{\Gamma}\frac{d^2\Gamma}{dx_g dx_w} = \left(\frac{\alpha_S C_F}{\pi}\right)\frac{1}{x_g^2(1-x_w)}\left[x_g - \frac{(1-x_w)(1-x_g)+x_g^2}{1-a}\right.$$
$$\left. \ldots + x_g \frac{(x_w + x_g - 1)^2}{2(1-a)^2} + \frac{2a(1-x_w)x_g^2}{(1-a)^2(1+2a)}\right]$$

where C_F represents the colour factor.

The logarithmic divergence associated with the emission of a single soft or collinear gluon means that such an emission is extremely likely. In contrast, *hard* gluon emission, where the gluon is emitted with large energy and hence a large angle between the gluon and weak current or bottom quark, is suppressed.

Parton Shower

We would like to consider the differential cross section for the top quark decaying to a multi-parton final state. From the above analysis we would expect to get logarithmic terms for each soft or collinear gluon emitted. Hence, the soft and collinear gluon emission represents a region of phase space for which higher order (α_S) processes are enhanced.

A large amount of gluon emission corresponds to a 'parton shower'. Thus we can say that a parton shower consisting of soft or collinear gluons is extremely likely. However hard gluon emission is suppressed by the denominator of the propagator(s).

The parton shower has its electromagnetic counterparts. For example, synchrotron radiation consists of coherent electromagnetic radiation beamed in the direction of the accelerated electron.

In electromagnetism, accelerated charged particles radiate photons; described by the photon-electron vertex in the theory of Quantum ElectroDynamics (QED). Similarly with the strong interaction, accelerated colour-carrying particles radiate gluons. In QCD, we have three (and four) gluon vertices in addition to the quark-gluon vertex, since the gluon vector field carries colour.

Thus each emitted gluon will itself radiate gluons and quarks, producing a cascade of emission; the parton shower. Indeed, for the rare event of a hard gluon being emitted in the top quark decay process, this too will initiate a parton shower; observed as a 'gluon jet'.

Parton Shower Approximation

Complete fixed order perturbative QCD analysis of top decay to multi-parton states is not practical. The work involved increases roughly factorially with the order in α_S [2].

The parton shower approximation has been developed to allow analysis of the *total* differential cross section in the regions of phase space for which emission is enhanced. In the soft or collinear limit the matrix for $t \to bWg^N$ can be effectively be factorised in terms of single gluon emission and the weak vertex. This allows the evolution of the parton shower off one of the quarks to be considered independently of the weak vertex.

The parton shower approximation gives the branching probability, $dP(q \to qg)$, for a parton to be emitted [3].

9) $$\frac{dP}{d\tilde{\kappa}dz} = \left(\frac{\alpha_S C_F}{\pi}\right)\frac{1}{2\tilde{\kappa}(1-z)}\left[1+z^2-\frac{2m^2}{z\tilde{\kappa}}\right]$$

The branching probability is based on the first-order matrix element for $t \to bWg$. The step-by-step evolution of the parton shower may be simulated using Monte Carlo methods. This gives us an approximate 'first-order' perturbative treatment of the parton shower to all orders of α_S.

Since it is based on the first-order matrix, divergences are still present. These are avoided by applying a lower cut-off for the shower [1].

The parton shower approximation considers showers off the top and bottom quark separately. It is formally valid for soft emission off the top quark and collinear emission off the bottom quark.

We therefore divide the phase space into three regions. The region of phase space corresponding to soft emission can be covered by a parton shower off the top quark. The region of phase space corresponding to collinear emission can be covered by a parton shower off the bottom quark. The remaining region of phase space, is called the 'dead region'.

In this paper, we aim to estimate the 'correction' to the parton shower approximation from integrating the differential cross section for the process $t \to bWg$ (eqn 8) over the dead region. The dead region necessarily includes the suppressed *hard* gluon emission; thus the first-order matrix should give a good approximation.

Kinematics

To define the dead region, we must first introduce new variables to describe the two parton showers.

We may express any general 4-momentum in terms of the parent parton momentum, p, a light-like 4-vector, n, and a transverse component, $q_{\perp i}$.

10) $$q_i = \alpha_i p + \beta_i n + q_{\perp i}$$
$$q_{\perp i}.p = q_{\perp i}.n = n^2 = 0$$

The coefficients α_i and β_i are dependent on the parent momentum, *p*, and our choice of *n*.

The evolution of the parton shower depends on the frame of observation [4]. We shall choose to observe the shower in the top rest frame. In this frame the collinear gluon emission from the 'acceleration' of the top quark will be beamed along the direction of the W boson. We choose the starting conditions for the respective showers off the top and bottom quark to be:

11) $$p = \begin{cases} p_t = m_t(1,0,0,0) \\ p_b = \frac{1}{2}m_t(1,0,0,1) \end{cases}$$
$$n = \tfrac{1}{2}m_t(1,0,0,-1)$$

The parent momentum for the shower off the bottom quark is the momentum of the massless bottom quark without gluon radiation. Thus, we are forced to align the weak current parallel to $\mathbf{p}_b$, corresponding to the constraint [1]:

12) $$\alpha_w - \frac{a}{\alpha_w} < 0$$

With our choice of p_t, p_b, and *n*, we find that q_i maps onto α_i in the same way for each shower.

13) $$\alpha_i = \frac{q_i.n}{p.n} \equiv 2\frac{q_i.n}{m_t^2};\ p.n = \tfrac{1}{2}m_t^2$$

Parton Shower variables

For $q^{(j)}$ corresponding to the *j*th quark in the parton shower, we define the momentum fraction, $z^{(j)}$, and relative transverse momentum, $\mathbf{p}_\perp^{(j)}$.

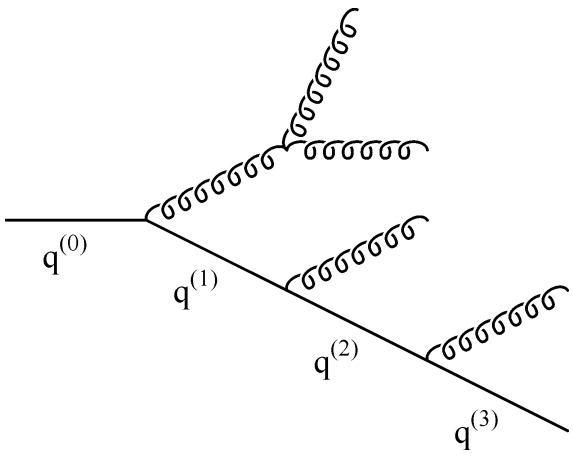

Figure 5, evolution of a parton shower

$$14)\qquad q^{(j)} = \alpha^{(j)} p + \beta^{(j)} n + q_\perp^{(j)}$$

$$15)\qquad z^{(j)} = \frac{\alpha^{(j)}}{\alpha^{(j-1)}}$$

$$16)\qquad \mathbf{p}_\perp^{(j)} = \mathbf{q}_\perp^{(j)} - z^{(j)} \mathbf{q}_\perp^{(j-1)}$$

To derive the dead region in Dalitz phase space, we must study the first stage of the respective parton showers.

For emission off the top quark (figures 3 & 6), the parton shower is placed before the weak vertex.

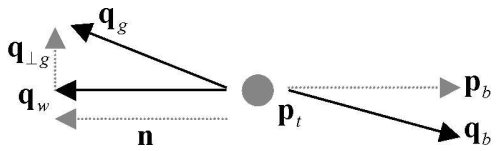

Figure 6, first stage of parton shower off top

$$17)\qquad \begin{aligned} q^{(0)} &= p_t \\ q^{(1)} &= q_w + q_b \\ z^{(1)} &= \alpha_w + \alpha_b \equiv 1 - \alpha_g = z_t \\ \mathbf{p}_\perp^{(1)} &= q_{\perp w} + q_{\perp b} \equiv -q_{\perp g} = \mathbf{p}_{\perp t} \end{aligned}$$

For bottom emission (figures 4 & 7), the parton shower is placed after the *W* vertex.

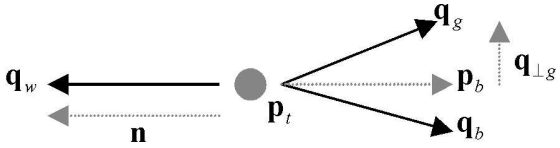

Figure 7, first stage of parton shower off bottom

$$18)\qquad \begin{aligned} q^{(0)} &= p_t - q_w \\ q^{(1)} &= q_b \\ z^{(1)} &= \frac{\alpha_b}{1-\alpha_w} = z_b \\ \mathbf{p}_\perp^{(1)} &= q_{\perp b} \equiv -q_{\perp g} = \mathbf{p}_{\perp b} \end{aligned}$$

Generally, these variables map differently onto phase space. However, in the rest frame of the top quark, momentum conservation requires that the three final state particles lie in the same plane. With our choices of *n* and *p* (eqn 11) the transverse direction is the same for both showers.

$$19)\qquad \mathbf{p}_{\perp t}^2 \equiv \mathbf{p}_{\perp b}^2 = \mathbf{p}_\perp^2$$

$$20)\qquad z_t \neq z_b$$

$$21)\qquad \kappa = \frac{\mathbf{q}_{\perp g}^2}{m_t^2} \equiv \frac{\mathbf{p}_\perp^2}{m_t^2}$$

The allowed phase space (eqn 5) coincides with real transverse momentum and positive coefficients, α, (positive energy). This is shown in figure A2 in the appendix.

$$22)\qquad \mathbf{p}_\perp^2 > 0\,;\ \alpha_b, \alpha_g \alpha_w > 0$$

For clarity we shall use the subscript *t* or *b* where necessary to distinguish between coordinates for the two showers. We emphasise that it is a coincidence that some of the shower coordinates have the same relations; based on our choice of initial conditions and the fact that we are only considering the first stage of the shower. We can map the coefficients onto the Dalitz variables:

$$23)\qquad x_g = \alpha_g + \frac{\kappa}{\alpha_g}$$

$$24)\qquad x_w = \alpha_w + \frac{a}{\alpha_w} - a$$

The dead region

We shall define the dead region using the evolution variable for each parton shower:

$$25)\qquad \tilde{q}^2 = \frac{\mathbf{p}_\perp^2}{z^2(1-z)^2} + \frac{m^2}{z^2}$$

This is derived from the propagator denominator of the appropriate Feynman diagram (figure 3 or 4), and modified to take into account angular ordering[1]. We shall work with a quantity proportional to this:

$$26)\qquad \begin{aligned} \tilde{\kappa}_t &= \frac{\tilde{q}_t^2}{m_t^2} = \frac{\kappa}{z_t^2\left(1-z_t^2\right)^2} + \frac{1}{z_t^2} \\ \tilde{\kappa}_b &= \frac{\tilde{q}_b^2}{m_t^2} = \frac{\kappa}{z_b^2\left(1-z_b^2\right)^2} \end{aligned}$$

These refer to the first stage of the shower. The variables will take different values at later branches of the shower. The evolution of an angular-ordered parton shower obeys [1]:

$$27)\qquad \tilde{q}^{(j+1)} < z^{(j)} \tilde{q}^{(j)}$$

This ensures that the evolution variable can only decrease from the starting value at the first stage of the shower. We can therefore define the dead region in terms of upper bounds on the evolution variable for first stage of each shower, $\tilde{\kappa}_{t\max}$ and $\tilde{\kappa}_{b\max}$. Showers initiated, satisfying these conditions, will not stray into the dead region.

$$28) \qquad 0 < \tilde{\kappa}_t < \tilde{\kappa}_{t\max}$$

$$29) \qquad 0 < \tilde{\kappa}_b < \tilde{\kappa}_{b\max}$$

The lower limit on the evolution variable corresponds to soft and collinear emission for the top and bottom showers respectively. As we increase $\tilde{\kappa}_{\max}$, the shower approximation fails.

Contour plots of $\tilde{\kappa}_t$ and $\tilde{\kappa}_b$ in Dalitz phase space are shown in figures A3 and A4 in the appendix. Interesting cases are where the contour touches the bottom of phase space. As our schematic plot indicates (figure A2), this point coincides with the α coefficients becoming complex. Using this condition, we derive the relevant contours, $\tilde{\kappa}_t = 3.66$ and $\tilde{\kappa}_b = 1.16$ [1]. Whether these values have any more significance than this is unclear. As the contour plot indicates, picking $\tilde{\kappa}_{b\max} > 1.16$ results in a disconnected dead region. These values represent sensible limits on the shower parameters, $\tilde{\kappa}_{t\max}$ and $\tilde{\kappa}_{b\max}$.

However, we have an additional constraint on these parameters. We clearly want to configure the parton showers so that the integral of the first-order differential partial cross section over the dead region is finite.

$$30) \qquad f(x_g, x_w) = \frac{1}{\Gamma}\frac{d^2\Gamma}{dx_g dx_w}$$

In the soft limit, we have a pole of second order with respect to x_g. To fully cover this singularity we require:

$$31) \qquad \left.\frac{\partial x_w(x_g, \tilde{\kappa}_t)}{\partial x_g}\right|_{\substack{x_g=0 \\ \tilde{\kappa}_t=\tilde{\kappa}_{t\max}}} = \left.\frac{\partial x_w(x_g, \tilde{\kappa}_b)}{\partial x_g}\right|_{\substack{x_g=0 \\ \tilde{\kappa}_b=\tilde{\kappa}_{b\max}}}$$

$$\Rightarrow \tilde{\kappa}_{b\max} = \frac{(1-a)^2}{\tilde{\kappa}_{t\max} - 1}$$

Integration over dead region

We wish to integrate the function $f(x_g, x_w)$ over the dead region defined by the parameter $\tilde{\kappa}_{t\max} > 1$. One might consider expressing the integral in terms of two one-dimensional integrals:

$$I = \int_D dx_g\, dx_w\, f(x_g, x_w) = \int_0^{1-a} dx_g \left\{ \int_{x_{w\min}(x_g, \tilde{\kappa}_{t\max})}^{x_{w\max}(x_g, \tilde{\kappa}_{t\max})} dx_w\, f(x_g, x_w) \right\}$$

This would then lend the problem to numerical integration using the Trapezium rule or Simpson's rule methods [5], which have convergence for *d*-dimensional integration:

$$32) \qquad \sigma_{\hat{I}(Trapz)} \propto \frac{1}{N^{\frac{2}{d}}}; \sigma_{\hat{I}(Simp)} \propto \frac{1}{N^{\frac{4}{d}}}$$

However, our numerical integration must contend with the soft singularity lying on the edge of the dead region. Applying a cutoff in x_g to avoid divergence would underestimate the integral. We might consider using an 'open' quadrature algorithm – one that does not explicitly evaluate the integrand at the end points.

However we also have the problem that our dead region is irregular. Splitting the integral into two one-dimensional integrals requires knowledge of the boundary of the dead region. An easier task would be to evaluate $\tilde{\kappa}_t$ and $\tilde{\kappa}_b$ in Dalitz phase space, to determine whether a given point is within the dead region.

We now consider estimating the integral using Monte Carlo methods. These treat the integral as an average over a probability distribution. We shall see that the rate of convergence for two-dimensional integral is inferior to the Trapezium and Simpson techniques mentioned above. However, Monte Carlo methods are ideally suited to complex boundaries; and the sampling may be configured to improve the efficiency of the algorithm.

Method: Monte Carlo Integration

In order to implement Monte Carlo integration we must employ rejection sampling and importance sampling [6]. We consider the integral of the differential cross section, $f(x_g, x_w)$, over the dead region, *D*, as the weighted average of a quantity, ϕ, over an area, *A*.

$$\begin{aligned} I &= \int_D dx_g dx_w f(x_g, x_w) \\ &= \int_A dx_g dx_w R(x_g, x_w) f(x_g, x_w) \\ &= Z_p \int_A dx_g dx_w \left(\frac{R(x_g, x_w) f(x_g, x_w)}{P'(x_g, x_w)} \right) P(x_g, x_w) \\ &\equiv Z_p \langle \phi \rangle_P \end{aligned}$$

where we define,

$$\phi(x_g, x_w) = \left(\frac{R(x_g, x_w) f(x_g, x_w)}{P'(x_g, x_w)} \right)$$

$$R(x_g, x_w) = \begin{cases} 1 \text{ if } (x_g, x_w) \in D \\ 0 \text{ if } (x_g, x_w) \notin D \end{cases}$$

$$P(x_g, x_w) = \frac{P'(x_g, x_w)}{Z_p}$$

$$Z_p = \int_A dx_g dx_w P'(x_g, x_w)$$

The function, $R(x_g, x_w)$, rejects points lying outside of the dead region, allowing us to integrate over an arbitrary area, *A*, which includes *D*. $P(x_g, x_w)$ is an arbitrary probability distribution function, normalised over the area, *A*. Z_P is the normalisation constant.

This reduces the problem to one of generating *N* samples $\{x_g, x_w\}$, over phase space area *A*, obeying the probability distribution $P(x_g, x_w)$.

$$33) \qquad \hat{I} = \frac{Z_P}{N} \sum_{\{x_g, x_g\}_P}^{N} \phi(x_g, x_w)$$

Appling the central limit theorem, we can estimate the standard deviation of our estimate:

$$34) \qquad \begin{aligned} I &\approx \hat{I} \pm \sigma_{\hat{I}} \\ \sigma_{\hat{I}} &= Z_P \frac{\sigma_\phi}{\sqrt{N}}; \sigma_\phi^2 = \langle \phi^2 \rangle - \langle \phi \rangle^2 \end{aligned}$$

$$\hat{\sigma}_{\hat{I}} = \frac{Z_P}{\sqrt{N}} \left[\left(\frac{1}{N} \sum_{\{x_g, x_g\}_P}^{N} \phi(x_g, x_w)^2 \right) - \left(\frac{1}{N} \sum_{\{x_g, x_g\}_P}^{N} \phi(x_g, x_w) \right)^2 \right]^{\frac{1}{2}}$$

In the limit of *N*, our estimate converges to the 'true' value:

$$35) \qquad \begin{aligned} &\lim_{N \to \infty} \{\sigma_{\hat{I}}\} = 0 \\ &\Rightarrow \lim_{N \to \infty} \{\hat{I}\} = I \end{aligned}$$

Thus we could adopt uniform sampling and achieve the required precision through sheer brute force (assuming that we have a good quality supply of random numbers!). However, the sample points nearest to the soft singularity contribute most to the integral. Therefore we should consider sampling more points from this region.

Our estimate also converges to the true value, in the limit:

$$36) \qquad \lim_{\phi \to 1} \{\sigma_\phi\} = 0$$

This would be trivially satisfied by setting the probability distribution proportional to the differential cross section ($P'(x_g, x_w) = f(x_g, x_w)$) and rejecting no points (*D*=*A*). However this simply moves the problem to evaluating the normalisation constant!

We shall use the probability distribution, $P(x_g, x_w)$, with parameters *e* and *e'* to allow optimisation. This samples near the soft singularity and can be analytically integrated over the area *A*.

$$37) \qquad P(x_g, x_w) = \frac{1}{Z_P} \left(\frac{1}{x_g^2 + \varepsilon^2} \right) \left(\frac{1}{1 - x_w + \varepsilon'} \right)$$

We can generate samples obeying this distribution by performing a Jacobian transformation on samples taken from a uniform distribution (details in Appendices B & C). We shall rely on the intrinsic random number generator in Fortran 95, which should be sufficient for our purposes.

Algorithm Results & Discussion

Monte Carlo integration algorithms were written in Fortran 95. Several versions of the program were made to perform different tests.

Monte Carlo algorithms employing skewed sampling, $P(x_g, x_w; e = e' = 0.1)$ and uniform sampling, $Q(x_g, x_w)$, were run for comparison. Figures 8 and 9 show the 'accepted' samples in the dead region contributing to the integral.

Figures 10 and 11 show the progress of the Monte Carlo algorithm with these two sampling distributions. In both cases we converge to the same value. Note that the value of the integral is quoted without the factor of $\alpha_S C_F \pi^{-1}$.

The estimated standard deviation for the algorithm running with skewed distribution is seen to follow the equation (34) as expected. However, our estimate of the standard deviation involves integrating the square of ϕ, which, in itself, is not a finite integral! Not surprisingly, it was found that for the uniform distribution the estimated standard deviation of ϕ increased with *N*.

Running the algorithm with large *N*, indicates that the skewed sampling method is more efficient than uniform sampling (Table 1). The algorithm run with uniform sampling with high *N* would be more affected by a poor random number generator, since it uses a greater percentage of the samples.

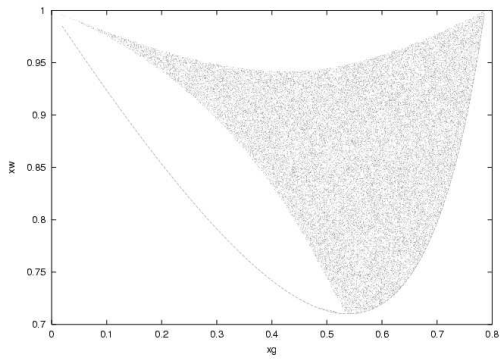

Figure 8, Uniform sampling

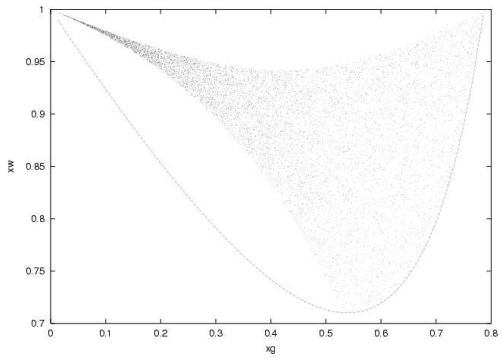

Figure 9, Skewed sampling (*e* = *e'* = 0.1)

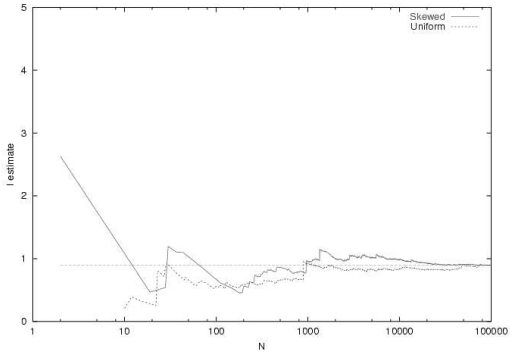

Figure 10, Estimate of I as algorithm progresses

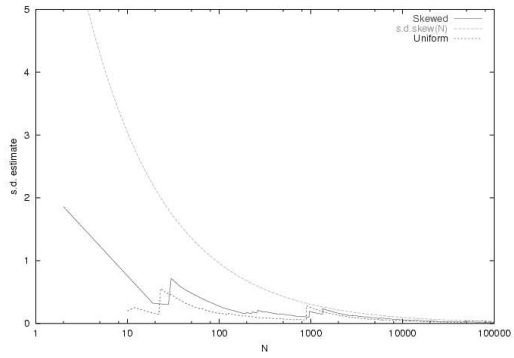

Figure 11, Estimated standard deviation

	Uniform sampling		Skewed sampling $e = e' = 0.1$		
%accepted	35.9 %	35.9 %	35.9 %	9.4 %	9.4 %
$Z_P \hat{\sigma}_\phi$	44.7	15.9	35.9	8.7	10.1
$\hat{I} \pm \hat{\sigma}_{\hat{I}}$	0.9031 ±0.0045	0.8980 ±0.001	0.9077 ±0.0076	0.9005 ±0.0009	0.9003 ±0.0010

Table 1; $N = 10^8$, $\tilde{\kappa}_{t\max} = 3.66$, $\tilde{\kappa}_{b\max} = 0.23$

To find the optimal settings, the algorithm was run repeatedly using different parameters (*e*,*e'*). The repeat runs (figure A5) broadly agree with the estimated standard deviation in the results.

The Monte Carlo algorithm was run over a range $\tilde{\kappa}_{t\max}$. The increase in the integrand with $\tilde{\kappa}_{t\max}$ in the lower range (figure 12/A6) corresponds to the increasing area of the dead region. In the limit of $\tilde{\kappa}_{t\max} \to 1^+$, the integrand approaches zero; corresponding to the parton shower off the bottom quark completely covering phase space.

However in the limit of high $\tilde{\kappa}_{t\max}$, the parton shower off the top quark is covering most of the phase space; yet the contribution over the dead region appears to approach a constant (figure 13/A7). However we take caution in the results for large $\tilde{\kappa}_{t\max}$ for which the uncertainty is significant.

At high $\tilde{\kappa}_{t\max}$, although the area of the dead region is very small, it is close to the collinear region. The soft and collinear singularities are still partially covered by the top and bottom showers, so perhaps one would expect the integrand to approach a limit.

These limiting cases are included for interest; certainly the parton shower would not be run with such parameters!

Results from individual runs are shown in Table 2. Running on a Pentium processor, the algorithm took about half an hour to compute a billion iterations.

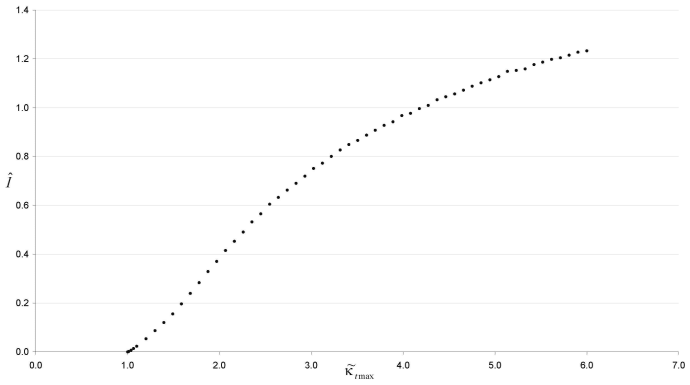

Figure 12, Integral over the dead region ($\tilde{\kappa}_{t\max}$)

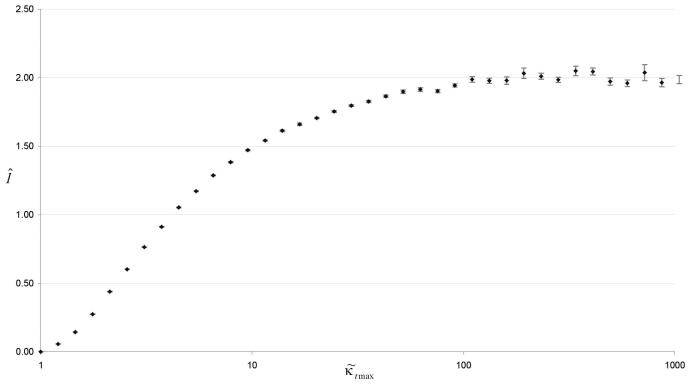

Figure 13, Integral over the dead region ($\tilde{\kappa}_{t\max}$)

$\tilde{\kappa}_{t\max}$	1.43	3.66	3.66
$\tilde{\kappa}_{b\min}$	1.43	0.232	0.232
%acceptance	4.8 %	9.4 %	9.4 %
$Z_P \hat{\sigma}_\phi$	2.59	9.64	9.60
$\hat{I} \pm \hat{\sigma}_{\hat{I}}$	0.13439 ±0.00008	0.9010 ±0.0003	0.9008 ±0.0003

Table 2; Skewed sampling, $e = e' = 0.1$, $N = 10^9$

Conclusions

We have found that the contribution to the total cross section from the matrix element ($t \to Wbg$) integrated over the dead region is of the order of unity (without the factor $\alpha_S C_F \pi^{-1}$).

The integral is dependent on our choice of $\tilde{\kappa}_{t\max}$, which defines the dead region in Dalitz phase space.

In choosing the most suitable $\tilde{\kappa}_{t\max}$, we must consider two factors; the accuracy of our correction and the validity of the parton showers.

The first-order matrix element gives us a reliable estimate for the correction. Our first-order treatment of the correction is valid in the region of phase space corresponding to hard emission. Therefore we wish to minimise the soft and collinear phase space falling within the dead region.

The parton shower approximation is most accurate when low maximum evolution parameters are chosen, corresponding to soft/collinear gluon emission. In these limits we would expect the branching probability to coincide with the first-order matrix element. Work into this was not completed.

The integral was calculated for the special case of $\tilde{\kappa}_{t\max} = \tilde{\kappa}_{b\max} = 1.43$. However, there is an intrinsic asymmetry between the two showers, due to the ratio of the parent quark masses. Additionally, we have chosen to view the parton showers in the top quark rest frame. This means that having equal evolution parameters for the two showers is not necessarily most suitable.

We contrast this with gluon radiation in the $\left(e^+e^- \to q\bar{q}\right)$ process, for which the only difference between the parent partons is the matter/antimatter asymmetry.

Acknowledgements

Sincere thanks to Bryan Webber for his patience with this project! Thanks also to Stefan Gieseke for a useful discussion regarding the context of the project.

References

1. Gieseke, Stephens, Webber. New Variables for Parton Showers. *Unpublished*, April 2002
2. Ellis, Stirling, Webber. QCD and Collider Physics. *Cambridge University Press* (1996)
3. Cacciari, Catani. Soft-gluon resummation for the fragmentation of light and heavy gluons at large x, [hep-ph/0107138]
4. Corcella, Seymour. Matrix element corrections to parton shower simulations of heavy quark decay. *Phys. Lett B* **442**, 417-426 (1998)
5. Press, Flannery, Teukolsky, Vetterling. Numerical Recipes. *Cambridge University Press* (1986)
6. Mackay, ed. M.Jordan. Introduction to Monte Carlo Methods. *A review paper in the proceedings of an Erice summer school*
7. Corcella *et al*. HERWIG 6: An event generator for hadron emission reactions with interfering gluons (including supersymmetric processes). *JHEP* **0101** (2001) [hep-ph/0011363]

Appendix A: Graphs

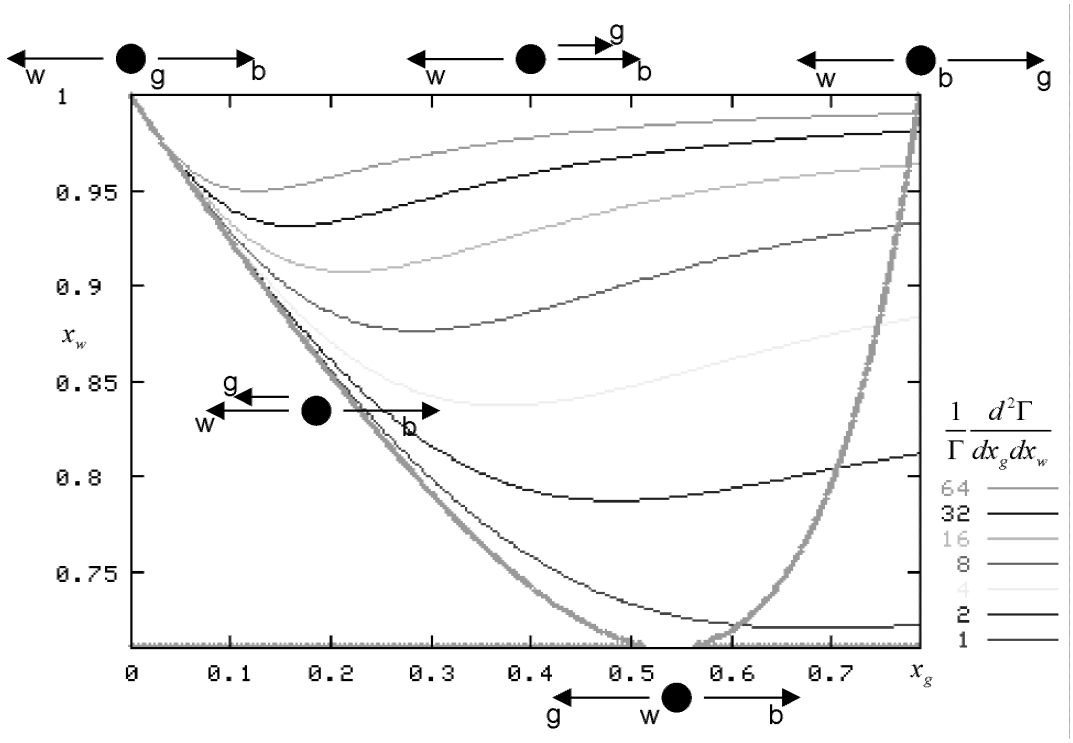

Figure A1, The behaviour of the first-order differential cross section over phase space

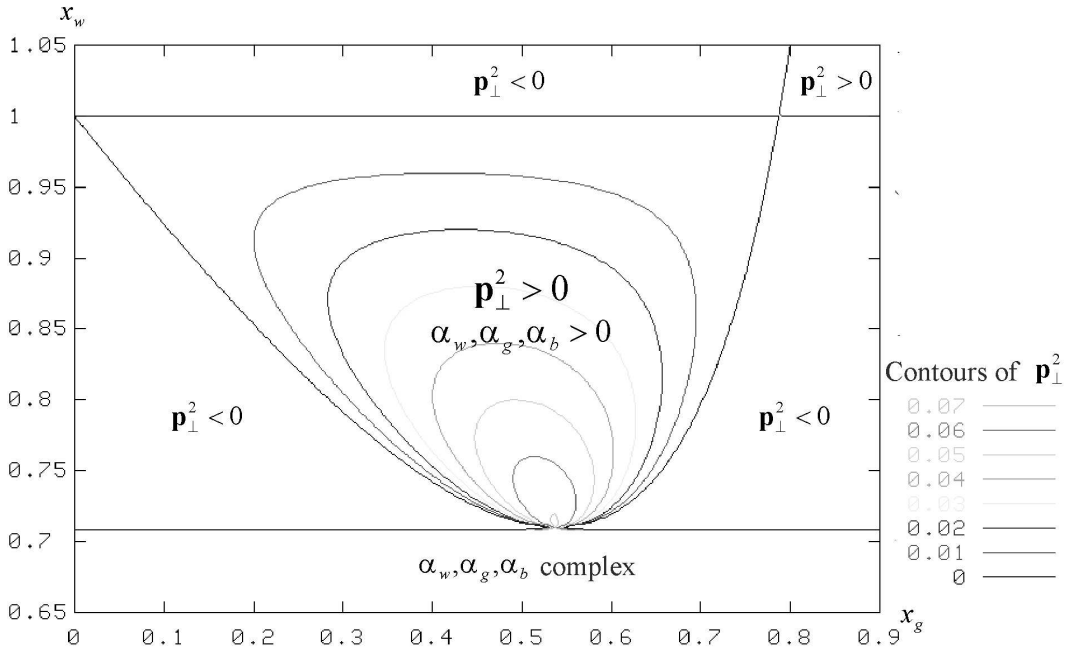

Figure A2, Parton shower variables over phase space

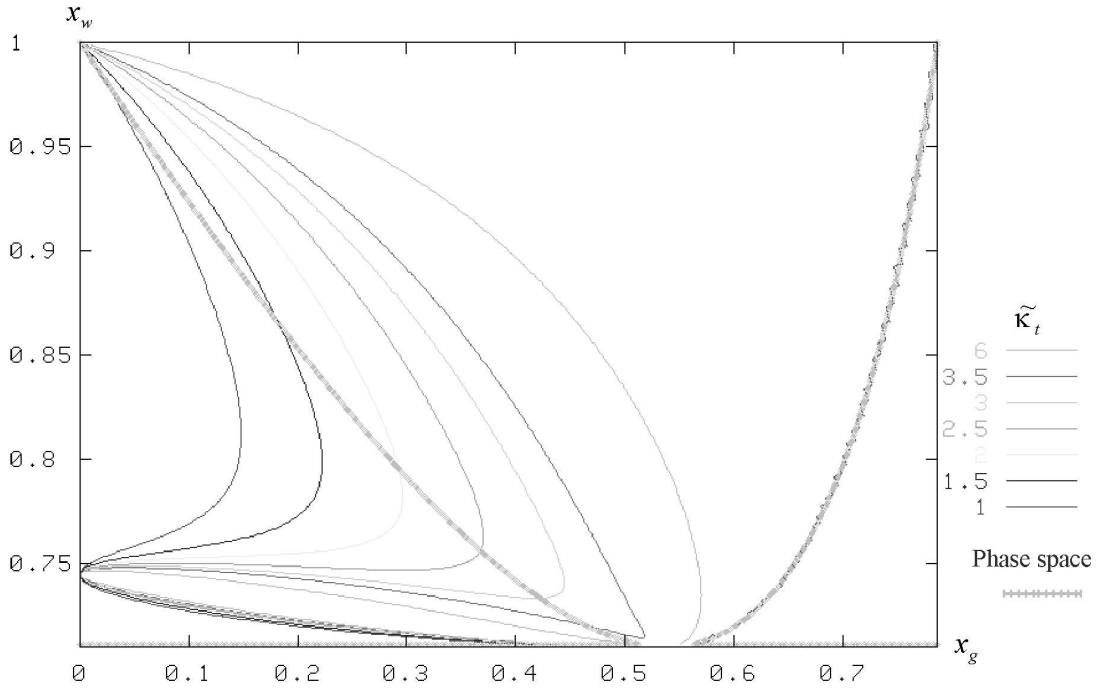

Figure A3, Contours of $\widetilde{\kappa}_t$ in Dalitz phase space

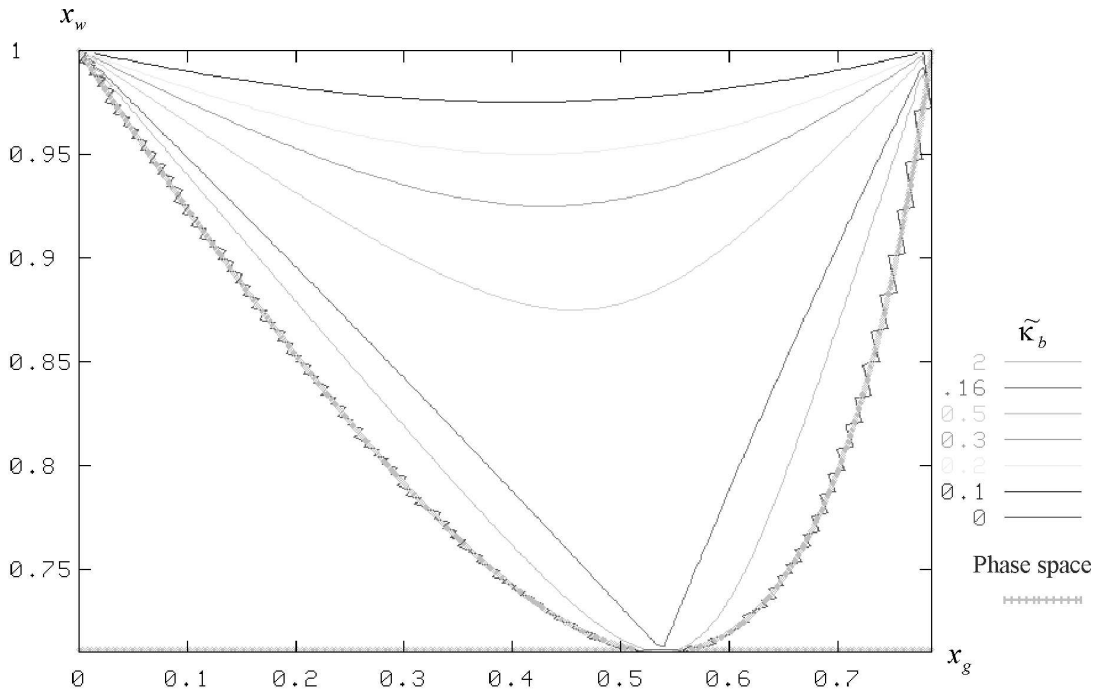

Figure A4, Contours of $\widetilde{\kappa}_b$ in Dalitz phase space

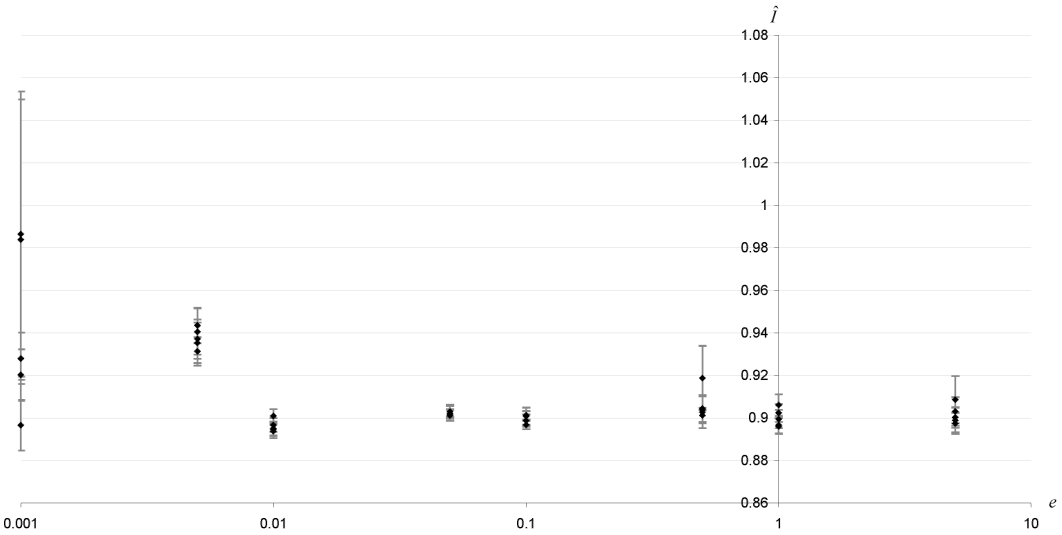

Figure A5, Results from different runs of the Monte Carlo algorithm

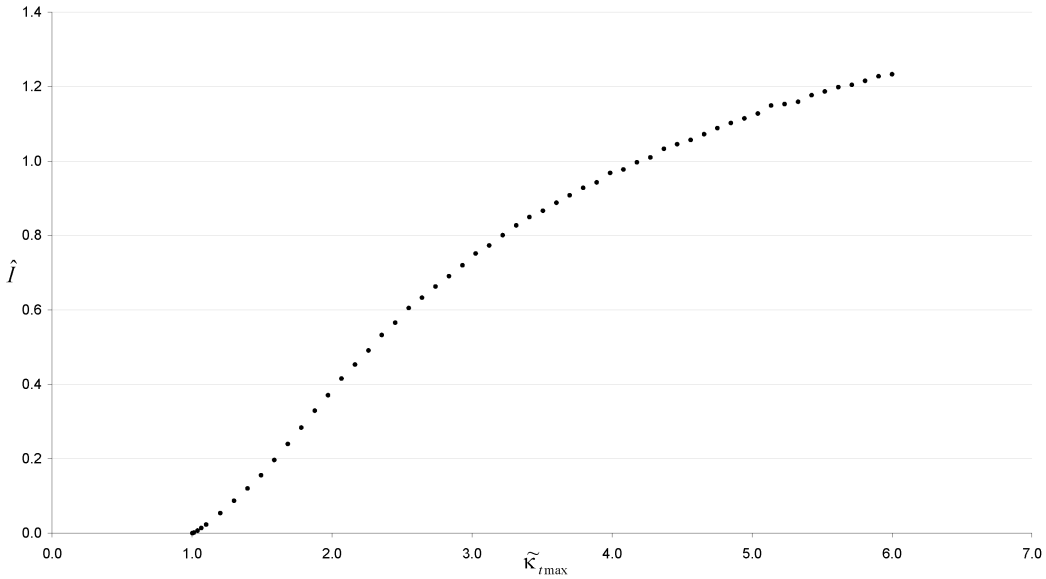

Figure A6, Integral over the dead region ($\widetilde{\kappa}_{t\max}$)

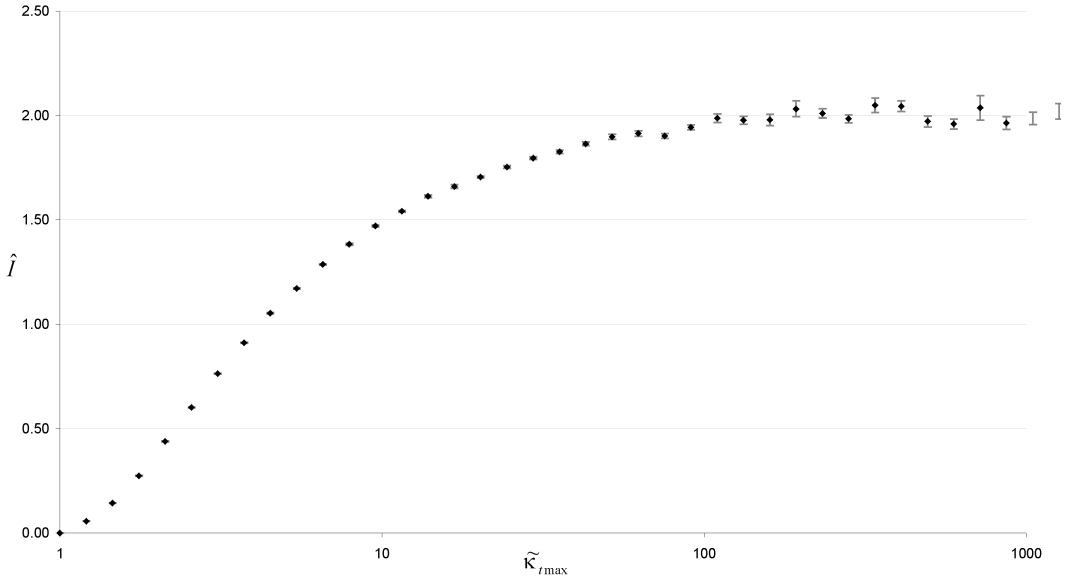

Figure A7, Integral over the dead region ($\tilde{\kappa}_{t\max}$)

Appendix B: Calculations

Mapping Dalitz variables onto parton shower variables

We may determine values of $\tilde{\kappa}_t$ and $\tilde{\kappa}_b$ and the other shower variables at any point in Dalitz phase space. From equation (24):

$$38) \qquad \alpha_w(x_g) = \tfrac{1}{2}(1+a) \pm \tfrac{1}{2}\sqrt{x_w^2 + 2ax_w - 4a + a^2}$$

This implies that alpha w is complex for

$$39) \qquad x_w^2 + 2ax_w - 4a + a^2 < 0$$

this coincides with the lower boundary of phase space (equation 5). α_w appears to be doubled-valued. However we choose the positive solution, believing this to satisfy equation (12).

Momentum conservation imposes the constraint:

$$40) \qquad \alpha_b + \alpha_g + \alpha_w = \frac{\kappa}{\alpha_b} + \frac{\kappa}{\alpha_g} + \frac{a}{\alpha_w}$$

From equations (23) and (39) we get:

$$41) \qquad \alpha_g(x_g, x_w) = \frac{(1-x_w) - x_g(1-\alpha_w(x_w))}{\alpha_w(x_w) - \dfrac{a}{\alpha_w(x_w)}}$$

For the top shower:

$$42) \qquad \begin{aligned} z_t(x_g, x_w) &= 1 - \alpha_g(x_g, x_w) \\ \tilde{\kappa}_t(x_g, x_w) &= \frac{x_g}{(z_t(x_g, x_w))^2 (1 - z_t(x_g, x_w))} \end{aligned}$$

For the bottom shower:

$$43) \qquad \begin{aligned} z_b(x_g, x_w) &= 1 - \frac{\alpha_g(x_g, x_w)}{1 - \alpha_w(x_g, x_w)} \\ \tilde{\kappa}_b(x_g, x_w) &= \frac{\kappa(x_g, x_w)}{[z_b(x_g, x_w)(1 - z_b(x_g, x_w))]^2} \end{aligned}$$

Jacobian Transformation of uniform sample

Consider the probability distribution:

$$44) \qquad P(x_g, x_w) = \frac{1}{Z_P}\left(\frac{1}{x_g^2 + \varepsilon^2}\right)\left(\frac{1}{1 - x_w + \varepsilon'}\right)$$

$$45)\quad \begin{aligned} Z_P &= \int_A dx_g\, dx_w \frac{1}{x_g^2+\varepsilon^2}\frac{1}{1-x_w+\varepsilon'} \\ &= \tfrac{1}{\varepsilon}\arctan\left(\frac{1-a}{\varepsilon}\right)\log\left(\frac{1-x_{w\min}+\varepsilon'}{\varepsilon'}\right) \end{aligned}$$

We wish to transform samples from a uniform deviate

$$46)\quad \{y,z\}_Q \rightarrow \{x_g, x_w\}_P$$

$$47)\quad \begin{aligned} Q(y,z) &= \frac{1}{Z_Q} \\ Z_Q &= \int_B dydz = (b'-a')(d'-c') \end{aligned}$$

Suppose that y is generated the range $[a',b']$; and z is generated the range $[c',d']$. We perform a Jacobian transformation:

$$48)\quad P(x_g,x_w)dx_g dx_w = \begin{vmatrix} \frac{\partial y}{\partial x_g} & \frac{\partial y}{\partial x_w} \\ \frac{\partial z}{\partial x_g} & \frac{\partial z}{\partial x_w} \end{vmatrix} .Q(y,x)dx_g dx_w$$

Choose two-to-two mapping with boundary conditions:

$$49)\quad \begin{aligned} &\{y,z\} \rightarrow \{x_g(y), x_w(z)\} \\ &(a',c') \rightarrow (0, x_{w\min}) \\ &(b',d') \rightarrow (1-a,1) \end{aligned}$$

We can also choose:

$$50)\quad Z_Q = Z_P$$

We solve,

$$51)\quad \frac{1}{Z_P}\frac{1}{x_g^2+\varepsilon^2}\frac{1}{1-x_w+\varepsilon'} = \frac{dy}{dx_g}\frac{dz}{dx_w}\frac{1}{Z_Q}$$

which is separable…

$$52)\quad \begin{aligned} x_g(y) &= \varepsilon\tan(y\varepsilon) \\ x_w(z) &= 1+\varepsilon'-e^{-z} \end{aligned}$$

Uniform sampling has parameters:

$$53)\quad \begin{aligned} a' &= 0 \\ b' &= \tfrac{1}{\varepsilon}\arctan\left(\frac{1-a}{\varepsilon}\right) \\ c' &= -\log(1-x_{w\min}+\varepsilon') \\ d' &= -\log(\varepsilon') \end{aligned}$$

Appendix C: Fortran Code

```
PROGRAM TopDecay
! 8th version. 3rd May 2002.
! This program integrates the differential cross section f over the dead region
! using samples from a skewed probability distribution
! slimmed down version.

implicit none

! declarations of variables
real (kind(1.d0)) :: xg, xw
real (kind(1.0d0)) :: kt_, kb_
real (kind(1.0d0)) :: sum_phi, sumsq_phi, sdphi, I, sdI

! declarations of parameters & dummy variables
real :: a, kt_max, , e, e_, xgmin, xwminmin, perc
real (kind(1.0d0)) :: a_, b_, c_, d_, Z
real (kind(1.d0)) :: kb_max
integer N, acc, rej
character(LEN=15) :: filename

! parameters and input values
parameter (a = 0.213)
Print *, ' kt_max'
Read *, kt_max
Print *, ' e'
Read *, e
Print *, ' e_'
Read *, e_
Print *, ' Total no. of samples (acc & rej)?'
Read *, N
Print *, ' Filename in which to store results?'
Read *, filename

! compute parameters for skewed probabilty distribution
xgmin = 1 - sqrt(a) ! xg coord of min of xw
xwminmin = 1 - xgmin + a * xgmin / ( 1 - xgmin)
Z  = (1 / e) * atan( (1-a)/e ) * log( (1- xwminmin + e_)/e_ )
a_ = 0
b_ = (1 / e) * atan ( (1 - a) / e)
c_ = -log ( 1 - xwminmin + e_)
d_ = -log (e_)

! open file to store record progress
open(1, file=filename, err=909, action='write', status='replace')
write(1,*) '# TOP QUARK DECAY IN DEAD REGION ', filename
write(1,*) '# '
write(1,*) '# Repeated integrations over range of different dead regions.'
write(1,*) '# aw+ used. Skewed distribution.'
write(1,*) '# ', kt_max0, ' < kt~max < ', kt_maxM
write(1,*) '# N = ', N
write(1,*) '# e = ', e
write(1,*) '# e_= ', e_
write(1,*) '# '
write(1,*) '# kt~max kb~max I sdI Z sdphi %acc/N'

kb_max = ( 1 - a )**2 / (kt_max - 1)

! start integration loop
acc=0
```

```
rej=0
sum_phi = 0
sumsq_phi = 0

! generate random point (xg,xw) in phase space
101 CONTINUE

CALL SAMPLE1(xg,xw)

! compute kt_ and kb_ using subroutine
CALL FUNCS(xg, xw, kt_, kb_)

! is point in dead region?
If ( (xw > xwmin(xg) ).and.( xw < 1 ).and.( kt_ > kt_max ).and.( kb_ > kb_max ) ) then

   ! if yes then, accept...
   acc = acc + 1
   sum_phi = sum_phi + f(xg,xw) / prob_(xg, xw)
   sumsq_phi = sumsq_phi + ( f(xg,xw) / prob_(xg, xw) )**2

   ! estimates after (acc+rej) iterations
   I = (Z / (acc + rej)) * sum_phi
   sdI = ( Z / sqrt(1.0*acc + 1.0*rej) ) * sqrt( ( ( sumsq_phi/(acc + rej) - ( sum_phi/(acc
+ rej) )**2 )**2)**0.5 )

else
   ! reject point
   rej = rej +1
end if

! if we have performed N calculations, then stop, otherwise continue
IF ((acc + rej) == N) then
   goto 202
else
   goto 101
end if

! Our final estimates for the integral and it's variance
202 CONTINUE
I = (Z / N) * sum_phi
sdI = ( Z / sqrt(N*1.0) ) * sqrt( sumsq_phi / N  - ( sum_phi / N )**2)
sdphi = sqrt( sumsq_phi / N - ( sum_phi / N )**2)
perc = 100 * (acc*1.0)/(N*1.0)

! display results on screen and write to file
write(1,*) kt_max, kb_max, I, sdI, Z, sdphi, perc
Print *, perc, '% of total ', N, ' samples accepted'
Print *, ' '
Print *, ' Z      =', Z
Print *, ' varphi = ', ( sumsq_phi / N - ( sum_phi / N )**2)
Print *, ' '
Print *, 'I = ', I, ' +/- ', sdI
Print *, '(missing factor of as * KF / pi)'
Print *, ' estimated accuracy: ', (100 * sdI / I), '%'
Print *, ' '


GOTO 303
! Error messages
909 STOP ' Problem with file.'

303 close (1)
```

```
Print *, ' Results stored in file, ', filename

CONTAINS
! internal subprograms

  SUBROUTINE SAMPLE1(xg,xw)
    ! generates sample (xg,xw) according to distribution prob(xg,xw) from uniform deviate
    ! arguments
    REAL (KIND(1.d0)), INTENT(OUT) :: xg, xw

    ! internal variables
    REAL (KIND(1.d0)) :: y, z
    REAL (KIND(1.d0)), DIMENSION(2) :: HARVEST

    ! we shall use intrinsic subroutine
    INTRINSIC RANDOM_NUMBER

    ! range of random co-ord to be generated:


    CALL RANDOM_NUMBER (HARVEST)
    y = ( b_ - a_ ) * HARVEST(1) + a_
    z = ( d_ - c_ ) * HARVEST(2) + c_

    ! transform variables (y,z) -> (xg,xw)
    xg = e * tan( y * e )
    xw = ( 1 + e_ ) - exp( -z )

  END SUBROUTINE SAMPLE1


  SUBROUTINE FUNCS(xg, xw, kt_, kb_)
    ! this internal subroutine returns the values of kt_ and kb_ for the point (xg,xw)
    ! aw(xg,xw) can take two values. The parameter q, defined in the main body of the
program, specfies which expression for aw to use.

    ! arguments of subroutine
    REAL (KIND(1.D0)), INTENT(IN) :: xg, xw
    REAL (KIND(1.D0)), INTENT(OUT) :: kt_, kb_

    ! internal variables
    REAL (KIND(1.D0)) :: aw, ag, zt, zb, k

    ! parameters a and q are defined in the program
    aw = 0.5*xw + 0.5*a + 0.5*sqrt(xw**2 + 2*xw*a + a**2  - 4*a)
    ag = (  ( 1 -xw ) - xg*( 1 - aw )  ) / ( aw - a / aw )

    ! parton shower from top quark
    zt = 1 - ag
    kt_ = xg / (  zt**2 * ( 1 - zt )  )

    ! parton shower from bottom quark
    zb = 1 - ag / ( 1 - aw )
    k = ag * ( xg - ag )
    kb_ = k / (  zb * ( 1 - zb )  )**2

  END SUBROUTINE FUNCS


  FUNCTION xwmin(xg)
    ! the lower bound of allowed phase space (xg,xw)
```

```
    ! declare function
    REAL (KIND(1.D0)) :: xwmin
    ! declare argument variable (we use same symbol as in main body)
    REAL (KIND(1.D0)), INTENT(IN) :: xg

    ! a is a parameter set in the main program body
    xwmin = 1 - xg + a * xg / ( 1 - xg)

  END FUNCTION xwmin


  FUNCTION f(xg,xw)
    ! differential cross section (1st order QCD)
    ! without factor of alpha s * Cf / pi

    ! declare function
    REAL (KIND(1.D0)) :: f
    ! declare argument variable
    REAL (KIND(1.D0)), INTENT(IN) :: xg, xw

    ! a is a parameter set in the main program body
    f = (1 / ( ( 1 - xw )* xg**2 ))  *  (  xg  -  ( ( 1 - xw )*( 1 - xg ) + &
         xg**2 )/( 1 - a )  +  xg * ( xw + xg - 1 )**2 / ( 2 * ( 1 - a )**2 )  + &
         ( 2 * a * ( 1 - xw )* xg**2 ) / ( ( 1 - a )**2 * ( 1 + 2*a ) )  )

  END FUNCTION f


  FUNCTION prob_(xg,xw)
    ! unnormalised probablity distribution

    ! declare function
    REAL (KIND(1.D0)) :: prob_

    ! declare argument variables
    REAL (KIND(1.D0)), INTENT(IN) :: xg, xw

    prob_ = (  1 / ( xg**2 + e**2)  )*(  1 / ( 1 - xw + e_)  )

  END FUNCTION prob_


END PROGRAM TopDecay
```